© 2015. Published by The Company of Biologists Ltd | Development (2015) 142, 185-195 doi:10.1242/dev.109652

RESEARCH ARTICLE

Molecular dissection of segment formation in the developing hindbrain

Charlotte Labalette[1,*,¶], Michel Adam Wassef[1,2,‡,¶], Carole Desmarquet-Trin Dinh[1], Yassine Xavier Bouchoucha[1,2], Johan Le Men[1,2,§], Patrick Charnay[1,] and Pascale Gilardi-Hebenstreit[1]**

ABSTRACT

Although many components of the genetic pathways that provide positional information during embryogenesis have been identified, it remains unclear how these signals are integrated to specify discrete tissue territories. Here, we investigate the molecular mechanisms underlying the formation of one of the hindbrain segments, rhombomere (r) 3, specified by the expression of the gene *krox20*. Dissecting *krox20* transcriptional regulation has identified several input pathways: Hox paralogous 1 (PG1) factors, which both directly activate *krox20* and indirectly repress it via Nlz factors, and the molecular components of an Fgf-dependent effector pathway. These different inputs are channelled through a single initiator enhancer element to shape *krox20* initial transcriptional response: Hox PG1 and Nlz factors define the anterior-posterior extent of the enhancer's domain of activity, whereas Fgf signalling modulates the magnitude of activity in a spatially uniform manner. Final positioning of r3 boundaries requires interpretation of this initial pattern by a *krox20* positive-feedback loop, orchestrated by another enhancer. Overall, this study shows how positional information provided by different patterning mechanisms is integrated through a gene regulatory network involving two cis-acting elements operating on the same gene, thus offering a comprehensive view of the delimitation of a territory.

KEY WORDS: Egr2, Fgf, Hox, Krox20, Nlz, Transcriptional enhancer, Segmentation, Rhombomere, Zebrafish

INTRODUCTION

The delimitation of specific territories – the shape, size and proportions of which are precisely defined and underlie subsequent morphogenesis and adult physiology – is an essential aspect of development (Lander, 2011; Meinhardt, 2009). The formation of these territories requires fine-tuned and robust genetic control and involves complex regulatory networks (Kicheva et al., 2012). A growing number of studies, including genome-wide analyses, indicates that enhancer elements constitute essential nodes in these networks, using various strategies to control gene expression and integrating multiple regulatory inputs (de Laat and Duboule, 2013; Shen et al., 2012; Spitz and Furlong, 2012). However, how enhancers actually combine these inputs to convey patterning information is still poorly understood.

The hindbrain is an attractive model to investigate the genetic control of territory delimitation in vertebrates. It is subject to a segmentation process that leads to the formation of seven to eight transversal domains along the anterior-posterior (AP) axis and is highly conserved among vertebrates (Gilland and Baker, 1993; Moens et al., 1998; Tumpel et al., 2009). These segments, called rhombomeres (r), constitute developmental units for neuronal differentiation, branchiomotor nerve organisation and neural crest specification (Lumsden, 1990; Lumsden and Keynes, 1989; Lumsden and Krumlauf, 1996). The mechanisms governing the delimitation of the different rhombomeres have not yet been fully unravelled, although abnormalities in their territory size are known to have severe consequences on vital functions (Rossel and Capecchi, 1999; Schneider-Maunoury et al., 1993; Swiatek and Gridley, 1993).

Several signalling pathways, as well as a number of transcription factors and adhesion/repulsion molecules, have been implicated in the control of segmentation (Moens and Prince, 2002; Tumpel et al., 2009). Of particular interest are the transcription factors Krox20 and Hox from paralogous group 1 (PG1), Hoxa1 and Hoxb1, which play essential roles in the development of the r3-r5 region. The *Krox20* (also known as *Egr2*) expression domains coincide with r3 and r5, and this gene has been shown to specify these rhombomeres (Schneider-Maunoury et al., 1997, 1993; Swiatek and Gridley, 1993; Voiculescu et al., 2001). Understanding *Krox20* regulation would therefore be a major step in deciphering the molecular basis of segment formation and hindbrain patterning. Hox PG1 genes are expressed from r3 to posterior regions and are required for normal development of r4 and r5 (Barrow et al., 2000; Gavalas et al., 1998; Makki and Capecchi, 2010; McNulty et al., 2005; Rossel and Capecchi, 1999; Wassef et al., 2008). The genetic relationships between *Krox20* and Hox PG1 genes appear complex. Krox20 represses Hox PG1 gene expression (Garcia-Dominguez et al., 2006; Giudicelli et al., 2001), whereas Hox PG1 factors also act as repressors of *Krox20*, as the knockdown of Hox PG1 proteins lead to posterior extension of r3 in both mouse and zebrafish embryos (Barrow et al., 2000; Gavalas et al., 1998; McClintock et al., 2002). Accordingly, expression of *Krox20* and Hox PG1 genes become rapidly exclusive in the r3-r5 region (Barrow et al., 2000; Gavalas et al., 1998; McClintock et al., 2002; Wassef et al., 2008). However, *Krox20* and *Hoxa1* cooperate for the development of r3 (Helmbacher et al., 1998), and Hox PG1 factors are required for the transcriptional activation of *Krox20* (McNulty et al., 2005; Wassef et al., 2008). The molecular basis of this dual action of Hox PG1 factors on *Krox20* expression has to date not been understood.

Two members of the Fibroblast growth factor (Fgf) family, namely Fgf3 and Fgf8, are released from the r3-r5 region (Aragon and Pujades, 2009; Maves et al., 2002; McKay et al., 1996; Walshe

[1]Ecole Normale Supérieure, Institut de Biologie de l'ENS (IBENS), Inserm U1024, CNRS UMR 8197, Paris F-75005, France. [2]Sorbonne Universités, UPMC Univ Paris 06, IFD, 4 Place Jussieu, Paris 75252, Cedex 05, France.
*Present address: Wellcome Trust Sanger Institute, Wellcome Trust Genome Campus Hinxton, Cambridge CB10 1SA, UK. ‡Present address: Institut Curie, Unité de Génétique et de Biologie du Développement, Paris 75005, France. §Present address: Inserm Transfert, Paris Biopark, 7 rue Watt, Paris 75013, France.
¶These authors contributed equally to this work

**Author for correspondence (patrick.charnay@ens.fr)

Received 3 March 2014; Accepted 7 November 2014

Development (2015) 142, 185-195 doi:10.1242/dev.109652

et al., 2002; Wiellette and Sive, 2003) and promote *Krox20* expression in r3 and r5 (Labalette et al., 2011; Marin and Charnay, 2000; Maves et al., 2002; Walshe et al., 2002). More precisely, changes in the level of Fgf signalling affect the sizes of r3 and r5, suggesting that Fgfs play a morphogenetic role in the hindbrain. However, the details of the molecular pathway linking Fgfs to *Krox20* have not yet been elucidated.

To investigate the molecular mechanisms underlying segment formation, we have previously searched for the cis-acting regulatory elements involved in the control of *Krox20* expression in the hindbrain. Three enhancers have been identified: A, B and C (Chomette et al., 2006). These elements orchestrate two different phases in *Krox20* expression. Enhancers B and C are involved in the initiation of *Krox20* expression. Enhancer B activity is restricted to r5, whereas enhancer C is highly active in r3 and r5, and at lower levels in r4 (Chomette et al., 2006). Neither enhancer B nor C requires the Krox20 protein itself. By contrast, enhancer A requires direct binding of the Krox20 protein for its activity, which governs a positive-feedback loop that amplifies the initiation signal and maintains *Krox20* expression (Bouchoucha et al., 2013; Chomette et al., 2006).

In the present study, we investigate the details of the molecular mechanisms underlying the formation of r3 in zebrafish. We have solved the long-standing issue about the paradoxical action of Hox PG1 factors, and we could identify the effectors of the Fgf-dependent molecular pathway through the analysis of different transcriptional pathways controlling *krox20* (*egr2b* – *Zebrafish* International Resource Center/ZFIN database) expression. Most importantly, we provide a comprehensive view of the regulatory process, showing how multiple and sometimes opposite instructions are channelled through enhancer C to define its extent and level of activity, and, together with the positive-feedback loop, shape *krox20* expression pattern and r3.

RESULTS

Antagonistic actions of Hox PG1 factors shape the initiation pattern of *krox20* along the AP axis

Several studies have shown that *krox20* expression can be either activated or repressed by Hox PG1 genes, but the basis of this apparent contradiction is not clear. One possible explanation is that different levels of Hox PG1 have different effects on *krox20* expression. To test this, we generated a zebrafish transgenic line, carrying a construct in which the *hoxb1a* gene is placed under the control of a heat shock promoter (*hsp:hoxb1a*). Using this system, ubiquitous ectopic *hoxb1a* expression can be obtained and its level controlled by the length of the heat shock (supplementary material Fig. S1). A heat shock of 5 min and 38°C, performed at 100% epiboly, does not affect the rate of cell proliferation in r3 (supplementary material Fig. S2) and leads to ectopic activation of *krox20* in r2, at a level similar to that in r3 (Fig. 1A,B; n=43 and 37, respectively). By contrast, longer heat shocks lead to a progressive reduction of the level of *krox20* mRNA in r2-r3 (Fig. 1C,D; n=44 and 46, respectively). Injecting increasing amounts of *hoxb1a* mRNA into one- to two-cell stage zebrafish embryos and observing different developmental stages confirmed this difference in activity of low and high *hoxb1a* levels (supplementary material Fig. S3). Analysis of endogenous *hoxb1a* expression revealed that *krox20* is not the only affected gene (supplementary material Fig. S4). Taken together, these experiments indicate that low levels or doses of Hoxb1a activate *krox20* expression, whereas higher levels/doses repress it.

To further investigate the link between Hox PG1 factors and *krox20*, we performed loss-of-function experiments by injecting morpholinos at the one- to two-cell stage. As *hoxb1a* and *hoxb1b* have partially redundant functions, we used morpholinos targeting both genes. At the one-somite stage (1s), *krox20* expression is

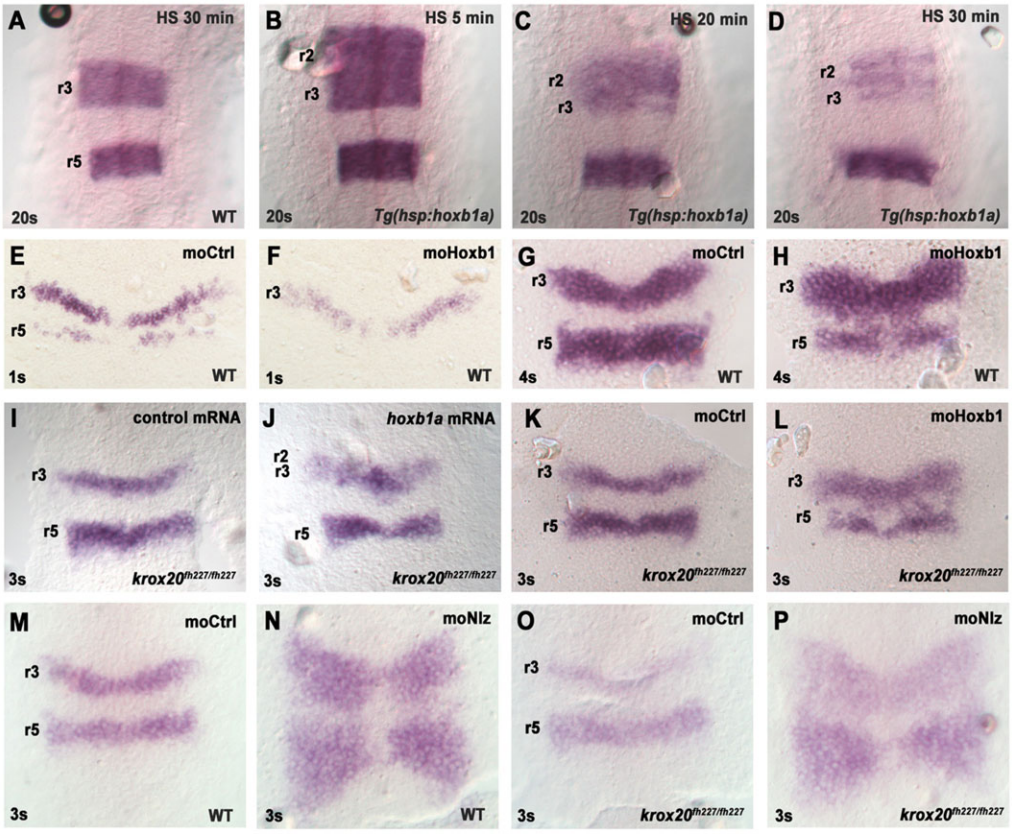

Fig. 1. Antagonistic actions of Hox PG1 and Nlz factors on *krox20* expression and initiation. All embryos were subjected to ISH with a *krox20* probe. (A-D) Wild-type (WT) or *Tg(hsp:hoxb1a)* embryos were heat-shocked (HS) for 5, 20 or 30 min at 100% epiboly and collected at 20s (three independent experiments). (E-H) WT embryos were injected with a control morpholino (moCtrl) or morpholinos for *hoxb1a* and *hoxb1b* (moHoxb1) and collected at 1s or 4s (three independent experiments). (I,J) *krox20*$^{fh227/fh227}$ mutant embryos were injected with 50 ng/µl of control or *hoxb1a* mRNAs and collected at 3s. (K,L) *krox20*$^{fh227/fh227}$ mutant embryos were injected with a control morpholino (moCtrl) or morpholinos for *hoxb1a* and *hoxb1b* (moHoxb1) and collected at 3s. (M-P) WT or *krox20*$^{fh227/fh227}$ mutant embryos were injected with a control morpholino or morpholinos for *nlz1 and nlz2* (moNlz) and collected at 3s. Embryos were flat-mounted with the anterior towards the top (see also Figs 2-6).

Development (2015) 142, 185-195 doi:10.1242/dev.109652

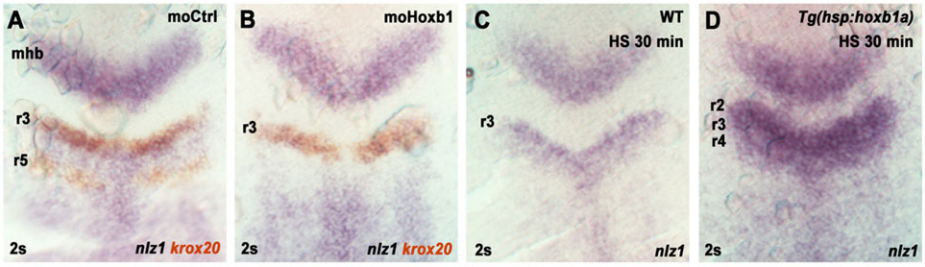

Fig. 2. Hox PG1 factors regulate *nlz1* expression. (A,B) Wild-type (WT) embryos were injected with a control morpholino (moCtrl) or morpholinos for *hoxb1a* and *hoxb1b* (moHoxb1), collected at 2s and subjected to *in situ* hybridization with *krox20* (orange) and *nlz1* (purple) probes. (C,D) WT and *Tg(hsp:hoxb1a)* embryos were heat-shocked (HS) for 30 min at 100% epiboly, collected at 2s and subjected to ISH for *nlz1* (three independent experiments). mhb, mid-hindbrain boundary.

reduced upon Hox PG1 knockdown (Fig. 1E,F; *n*=33 and 36, respectively). However, at 4s, normal levels of expression are re-established in r3 in the morphants and, in addition, numerous *krox20*-positive cells are observed in the r4 territory (Fig. 1G,H; *n*=58 and 83, respectively). These data suggest that Hox PG1 proteins are required for *krox20* activation in r3, but are also involved in its repression in r4. Furthermore, as the initial rostral border of Hox PG1 gene expression is in r3 (Makki and Capecchi, 2010; Wassef et al., 2008), these data suggest that these factors are limiting and are involved in setting the anterior boundary of *krox20* expression.

As *krox20* expression involves initiation and autoregulation phases, we investigated how initiation is affected by modifications in Hox PG1 levels. To study initiation without the confounding effects of autoregulation, we made use of an allele, *krox20*^{fh227} (Monk et al., 2009), which carries a point mutation in the *krox20* coding sequence, thus preventing the establishment of the autoregulatory loop (Bouchoucha et al., 2013). Similar to the effect observed in wild-type embryos (supplementary material Fig. S3B), injection of *hoxb1a* mRNA in *krox20*$^{fh227/fh227}$ embryos leads to an increase in the level of *krox20* expression and to a rostral extension of its anterior expression domain (Fig. 1I,J; *n*=51 and 21, respectively). Upon Hox PG1 knockdown in *krox20*$^{fh227/fh227}$ embryos, *krox20*-positive cells are observed in the r4 domain, and the r3 domain of *krox20* expression is extended caudally at the expense of r4 (Fig. 1K,L; *n*=79 and 28, respectively). These data establish that both activator and repressor activities of Hox PG1 proteins affect the initiation phase of *krox20* transcription in the r2-r4 region.

Nlz1 mediates Hox PG1 repression of *krox20*

We have previously shown in the mouse that the activation of *krox20* initiation by Hox PG1 factors involves direct binding of these proteins to enhancer C, which controls the initiation of *krox20* expression in r3 (Wassef et al., 2008). For the repressive activity of Hox proteins, we hypothesized that they act indirectly, and searched for possible mediators. Nlz factors (Nlz1 and Nlz2 in zebrafish; Znf703, Znf503 – Zebrafish International Resource Center) repress *krox20* (Hoyle et al., 2004; Nakamura et al., 2008; Runko and Sagerström, 2003, 2004), and we investigated whether they act at the level of initiation. A set of four morpholinos has been previously developed to knock down Nlz function (Hoyle et al., 2004). Injection of these morpholinos into wild-type embryos leads to posterior extensions of both *krox20* expression domains (Fig. 1M,N; *n*=58 and 62, respectively), as observed previously (Hoyle et al., 2004). The phenotype is very similar in *krox20*$^{fh227/fh227}$ embryos (Fig. 1O,P; *n*=25 and 28, respectively), suggesting that Nlz factors repress the *krox20* initiation phase in r4. To identify which Nlz protein is involved in *krox20* repression, we performed individual knockdown experiments for *nlz1* and *nlz2* (*znf703*, *znf503* – Zebrafish International Resource Center). Nlz2 morpholinos had little effect alone, whereas Nlz1 morpholinos led to a posterior extension of the r3 domain of *krox20* expression, largely recapitulating the effects observed with combined morpholinos (supplementary material Fig. S5). This indicates that the main player in the repression of *krox20* is Nlz1.

We then investigated whether the expression of *nlz1* is controlled by Hox PG1 factors. A detailed analysis of *nlz1* expression has been previously performed by Runko and Sagerström (2003). By tailbud stage, *nlz1* expression covers a large domain from the caudal end of the embryo to approximately the r3/r4 boundary. During early somitogenesis, this expression extends into r3. Morpholino knockdown of Hox PG1 proteins leads to a severe reduction in *nlz1* expression in the r3/r4 region at 2s (Fig. 2A,B; *n*=12 and 20, respectively). Conversely, ectopic expression of *hoxb1a* results in a major increase in the level of *nlz1* expression and to a rostral extension of the domain beyond r2 (Fig. 2C,D; *n*=16 and 19, respectively). Together, these data indicate that *nlz1* is under positive control of Hox PG1 proteins in the r3/r4 region, consistent with Nlz1 being an effector of Hox PG1 repression of *krox20*.

To further investigate this possibility, we performed an epistasis analysis. If Hox PG1 genes repress *krox20* by activating *nlz*, the repressive effect of *hoxb1a* overexpression should be prevented by knocking down Nlz. Indeed, when Hoxb1a gain-of-function and Nlz knockdown are combined, we observe a high level of *krox20* expression in almost the entire r2-r5 region (Fig. 3). Further corroborating the role of Nlz as an effector is the expression of *krox20* in r2, where *nlz1* is normally not expressed at early somitogenesis stages (Runko and Sagerström, 2003), and where Nlz knockdown has no effect on *krox20* expression under normal circumstances. In this rhombomere, *hoxb1a* misexpression leads to *nlz1* activation (Fig. 2D) and low *krox20* expression levels (Fig. 3A,B,E,F; *n*=16, 29, 24, 18, respectively), resulting from a combination of ectopic activation and repression. If *nlz* expression is prevented, a high level of *krox20* expression is observed, indicating that the gene has been de-repressed (Fig. 3C,D,G,H; *n*=19, 16, 43, 33, respectively). These analyses indicate that the repression of *krox20* expression by Hox PG1 proteins is mediated by Nlz1.

Hox PG1 and Nlz1 factors pattern the activity of enhancer C

If Hox PG1 and Nlz factors control the pattern of initiation of *krox20* in r3, they are likely to act through enhancer C. To test whether these factors control enhancer C activity, we generated a reporter transgenic line, *Tg(*cC*:gfp)*, carrying the *gfp* reporter gene under the control of chick enhancer C. The onset of *gfp* expression occurs around 95% epiboly in a narrow transversal domain (Fig. 4A). At 100% epiboly, the activity of enhancer C overlaps with prospective r3 (anterior domain of expression of *krox20*), but also extends into prospective r4 at a lower level (Fig. 4B,E). This pattern of expression is maintained until 5s, with the domain of enhancer C activity progressively extending caudally to reach r5 (Fig. 4C,D,F,G).

Development (2015) 142, 185-195 doi:10.1242/dev.109652

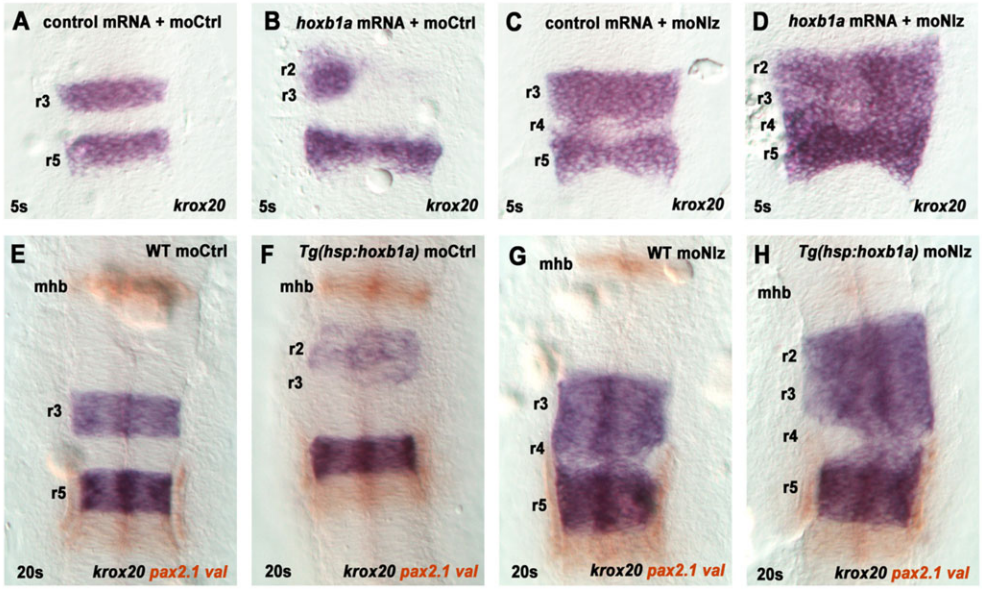

Fig. 3. Nlz factors mediate Hox PG1 repression of *krox20*. (A-D) Wild-type (WT) embryos were co-injected with 50 ng/µl of *hoxb1a* or *cherry-h2b* (control) mRNAs, together with either a control morpholino (moCtrl) or morpholinos for *nlz1 and nlz2* (moNlz). Embryos were collected at 5s and subjected to *in situ* hybridization with a *krox20* probe. (E-H) WT or *Tg(hsp:hoxb1a)* embryos were injected with either moCtrl or moNlz, heat-shocked for 30 min at 100% epiboly, collected at 20s and subjected to ISH with *krox20* (purple) and *pax2.1+val* (orange) probes. mhb, mid-hindbrain boundary.

Activity of enhancer C in r4 is surprising, as *krox20* is not expressed in this rhombomere under normal conditions. This is neither due to a position effect on the transgene nor to a species peculiarity, as the same pattern is observed (1) with two other lines carrying the same transgene (C. Labalette, unpublished); (2) in transient zebrafish transgenic embryos carrying *gfp* under the control of the zebrafish enhancer C (J. Le Men, unpublished); and (3) in mouse transgenic lines (Chomette et al., 2006). Therefore, the activity of the transgenic enhancer C in r4 is likely to reflect an intrinsic aspect of *krox20* regulation, which is revealed by expression of the gene in this rhombomere under several circumstances (Hoyle et al., 2004; Labalette et al., 2011; Runko and Sagerström, 2003) and is modified when the enhancer is present on a transgene.

We then tested whether Hox PG1 and Nlz factors regulate enhancer C activity. Hox PG1 knockdown leads to a severe reduction of enhancer activity (Fig. 4H,I; n=66 and 97, respectively), whereas ectopic expression of *hoxb1a* increases enhancer activity, in particular in the r2/r3 region (Fig. 4J,K; n=30 and 34, respectively). Nlz knockdown leads to a posterior extension of the domain of activity (Fig. 4L,M; n=16 and 17, respectively). These data indicate that Hox PG1 and Nlz factors affect the pattern and domain of enhancer C in a manner comparable to their effect on

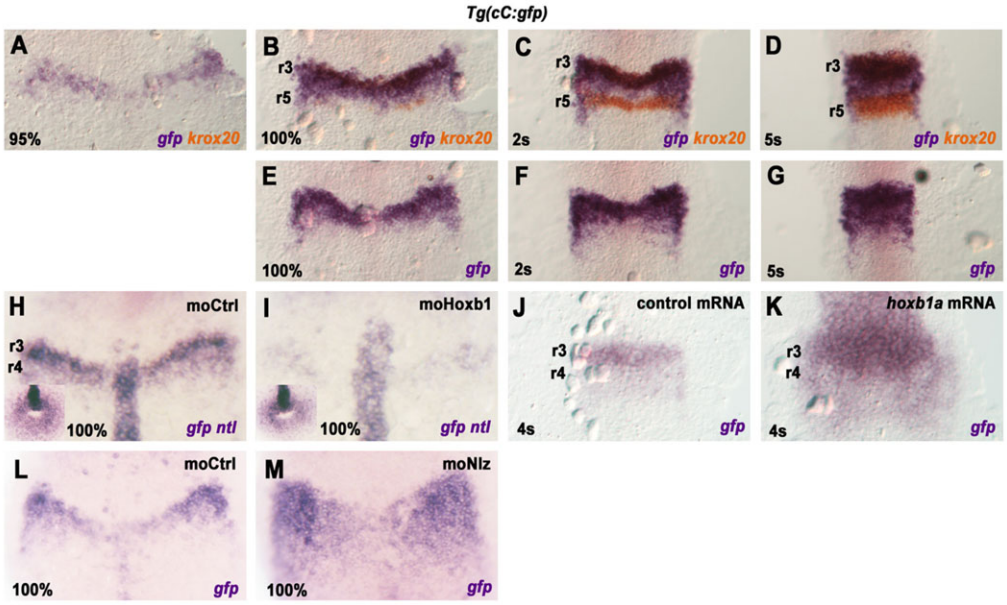

Fig. 4. Dynamics of enhancer C activity and its regulation by Hox PG1 and Nlz factors. (A-G) Time-course analysis of enhancer C activity. The *Tg(cC:gfp)* line was analysed by double ISH with *gfp* (purple) and *krox20* (orange) probes, at the indicated stages (A-D). Single ISH was also performed with the *gfp* probe (E-G). (H,I) *Tg(cC:gfp)* embryos were injected with a control morpholino (moCtrl) or morpholinos for *hoxb1a* and *hoxb1b* (moHoxb1), and subjected to ISH with *gfp* and *ntl* probes at 100% epiboly (three independent experiments). The insets show tailbud views of the embryos, allowing the developmental stage to be evaluated by extent of tailbud closure. (J,K) *Tg(cC:gfp)* embryos were injected with control or *hoxb1a* mRNA and subjected to ISH with a *gfp* probe at 4s (three independent experiments). (L,M) *Tg(cC:gfp)* embryos were injected with a control morpholino or morpholinos for *nlz1* and *nlz2* (moNlz), and subjected to ISH with a *gfp* probe at 100% epiboly.

Development (2015) 142, 185-195 doi:10.1242/dev.109652

the initiation of *krox20* itself, suggesting that the enhancer mediates the regulatory action of these factors on *krox20*.

Enhancer C mediates Fgf regulation of *krox20* in r3-r4

Fgf signalling is also involved in the patterning of *krox20* expression and in determining the size of r3 (Labalette et al., 2011; Maves et al., 2002; Walshe et al., 2002). However, its downstream effectors are poorly understood. We have previously shown that enhancer C is sensitive to changes in Fgf signalling (Labalette et al., 2011). With the *Tg(cC:gfp)* line, we performed a detailed analysis of the response of this element to Fgf input. *Tg(cC:gfp)* embryos treated from shield stage with the Fgf receptor inhibitor SU5402 have decreased enhancer C activity compared with control, vehicle-treated embryos (Fig. 5A,B; *n*=28 and 27, respectively). By contrast, Fgf gain-of-function by knockdown of Spry4, an Fgf negative-feedback regulator, leads to general enhancement of enhancer C activity in presumptive r3-r4 (Fig. 5C,D; *n*=30 and 24, respectively). Together, these results indicate that enhancer C activity is positively regulated by Fgf signalling, suggesting that this element mediates Fgf control of *krox20* expression in r3-r4.

Sp5l/Bts1 directly mediate Fgf regulation of enhancer C

Fgf signalling positively regulates the expression of the transcription factor Sp5l, which is required for *krox20* expression in r3 (Sun et al., 2006). To investigate whether Sp5l directly controls enhancer C activity, we searched for potential Sp5l-binding sites within the DNA sequence of enhancer C. We found one sequence that matches the consensus binding motif of the Sp family (Harrison et al., 2000) and is conserved among vertebrates (supplementary material Fig. S6). A deleterious double-point mutation (Berg, 1992; see also supplementary material Fig. S6) in this putative Sp5l-binding site resulted in a drastic decrease in reporter activity in three transgenic lines [*Tg(cCmutSp:gfp)*; Fig. 5E,F; and C. Labalette, unpublished]. To test whether the Sp site on enhancer C is involved in the response to Fgf signalling, embryos from one of the *Tg(cCmutSp:gfp)* lines were treated with SU5402 from shield stage onward. Levels of *gfp* are low in both control and SU5402-treated embryos (Fig. 5I,J; *n*=25 and 33, respectively). Furthermore, Spry4 knockdown does not significantly increase the activity of the mutant enhancer C (Fig. 5K,L; *n*=19 and 21, respectively). We conclude that mutation of the putative Sp site renders the element unresponsive to variations in Fgf signalling. This suggests that this sequence motif mediates Fgf regulation of enhancer C.

To determine whether Sp5 factors directly bind enhancer C, we first performed gel retardation experiments with nuclear extracts. These had been prepared from transfected COS-7 cells expressing an HA-tagged version of mouse Sp5. An oligonucleotide carrying the Sp site was specifically retarded and could be supershifted with an anti-HA antibody (Fig. 6A), indicating direct binding. We next tested whether Sp factors regulate enhancer C. A pTol2 plasmid carrying *sp5l* cDNA under the control of the *hsp* promoter (*pTol2-hsp:sp5l*) was injected into *Tg(cC:gfp)* embryos, which were then heat-shocked at 95% epiboly. Ectopic *sp5l* expression results in an upregulation of element C activity in the r3-r4 domain (Fig. 6B,C; empty vector, *n*=25; and ectopic *sp5l*, *n*=22). Interestingly, although *sp5l* is expected to be overexpressed in the entire embryo, enhancer C activity is only increased in its normal domain. Furthermore, overexpression of *sp5l* in the *Tg(cCmutSp:gfp)* line did not cause any increase in the activity of the mutant element C lacking the Sp site (Fig. 6D,E; *n*=31 and 24, respectively).

To investigate whether endogenous Sp5 factors are required for enhancer C activity, we performed a simultaneous knockdown of the two zebrafish *sp5* homologs, *sp5l* and *bts1*, in the *Tg(cC:gfp)* line. Whereas 90% of the transgenic embryos co-injected with specific morpholinos against Sp5l and Bts1 show a low level of reporter expression (Fig. 6G; *n*=73), more than 80% of the embryos injected with control morpholinos carrying mismatch mutations express the reporter at a high level (Fig. 6F; *n*=51), thus supporting the involvement of these factors. The defect in reporter expression was rescued in 55% of transgenic embryos co-injected with *sp5l* mRNA (Fig. 6I; *n*=20), whereas 77% of embryos co-injected with Cherry mRNA still presented a low level of reporter activity (Fig. 6H; *n*=7). In addition, if Sp factors transduce the Fgf signal to regulate element C, Sp5l should rescue enhancer C activity upon a loss of Fgf signalling. Exposure of *Tg(cC:gfp)* embryos to SU5402 severely reduces the activity of element C (Fig. 6J,K; *n*=28 and 35, respectively; Fig. 6N), and *sp5l* gain-of-function efficiently rescues this activity (Fig. 6L,M; *n*=29 and 32, respectively; Fig. 6N; Fisher's Exact Test, $P<0.05$).

In summary, Fgfs regulate *sp5l* (Sun et al., 2006), *sp5l* and *bts1* are required for enhancer C activity, Sp5 factors bind to an Sp site involved in enhancer C regulation by Fgf, and *sp5l* rescues element

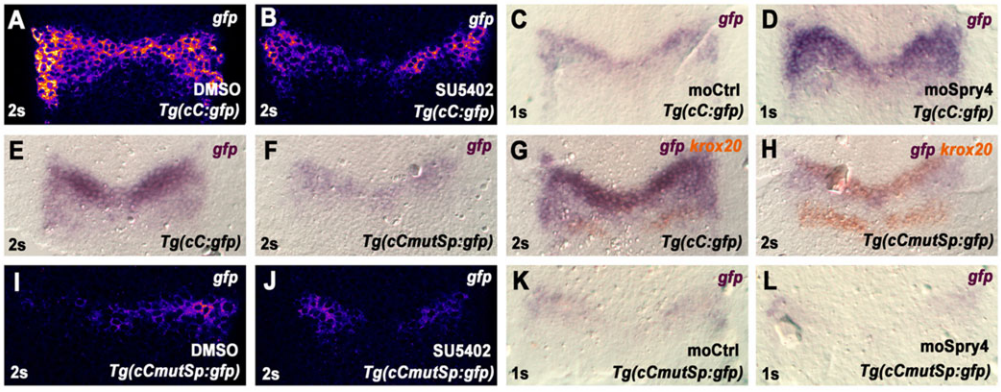

Fig. 5. Regulation of enhancer C activity by Fgf signalling. (A-D) *Tg(cC:gfp)* embryos were treated with control DMSO carrier or SU5402 from the shield stage (A,B), or injected with a control morpholino (moCtrl) or a morpholino for *spry4* (moSpry4), and analysed by ISH for *gfp* (three independent experiments). (E-H) Analysis of enhancer C activity in *Tg(cC:gfp)* and *Tg(cCmutSp:gfp)* embryos by single (E,F) or double (G,H) ISH for *gfp* (purple) and *krox20* (orange) at 2s. (I-L) *Tg(cCmutSp:gfp)* embryos were treated with DMSO carrier or SU5402 from the shield stage (I,J), or injected with a control morpholino (K) or a morpholino for *spry4* (S), and analysed by ISH for *gfp* (three independent experiments). In A,B,I,J, coloration reactions were performed with the Fast Red fluorescent compound to allow for quantification. ISHs were carried out in parallel on siblings under identical conditions.

Development (2015) 142, 185-195 doi:10.1242/dev.109652

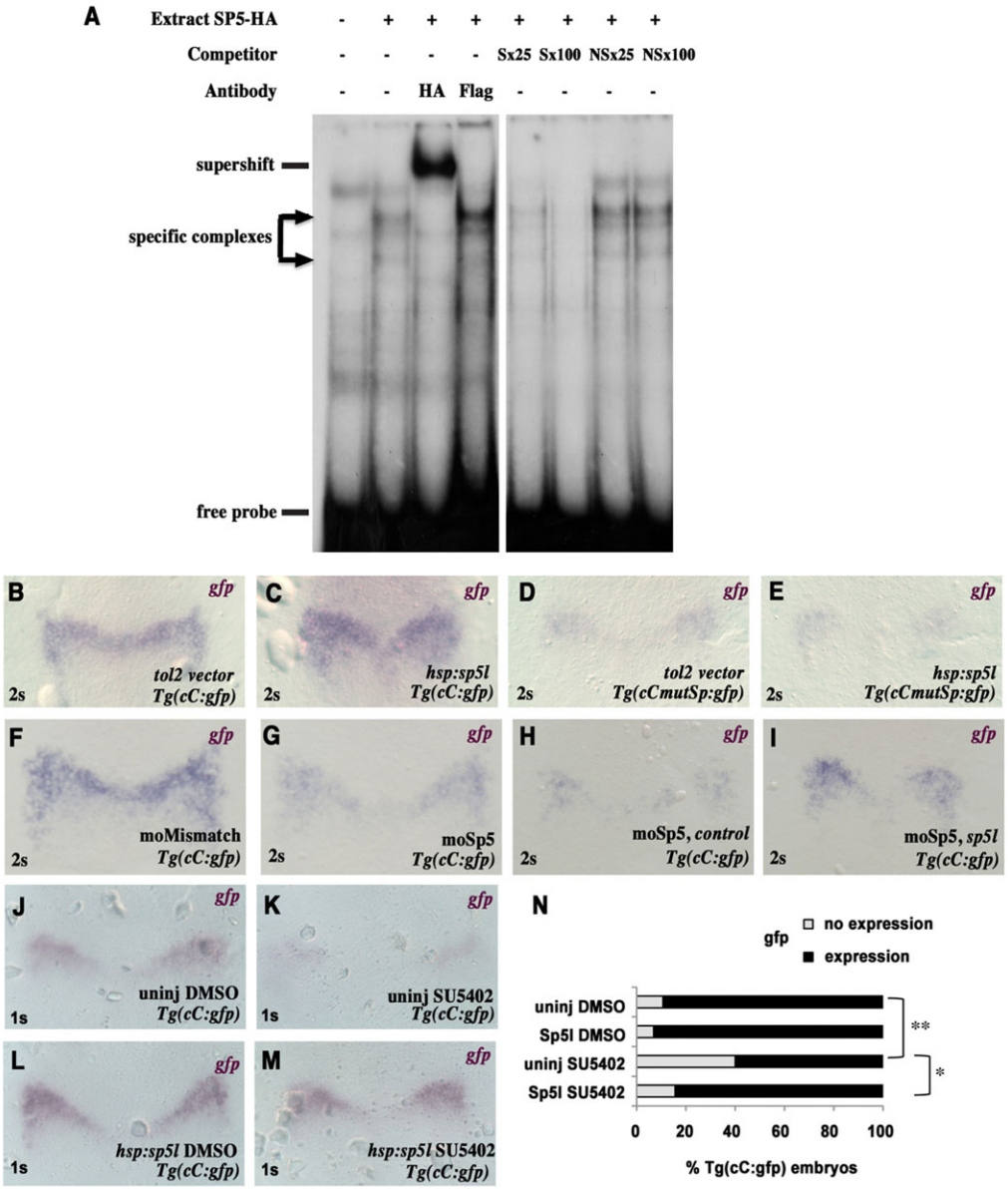

Fig. 6. Sp5 factors mediate Fgf signalling on enhancer C. (A) Gel retardation analysis of the binding of an HA-tagged SP5 protein to an oligonucleotide carrying the Sp site from element C. Antibodies against HA or Flag, and specific (S) or non-specific (NS) oligonucleotide competitors (25- or 100-fold molar excess with respect to the probe) were added as indicated. The positions of specific complexes (arrows), a supershifted complex and the free probe are indicated. (B-E) *Tg(cC:gfp)* or *Tg(cCmutSp:gfp)* embryos were injected either with a control plasmid (*tol2* vector) or an *sp5l* expression vector (*hsp:sp5l*) and heat-shocked for 10 min at 95% epiboly. ISH for *gfp* was performed at 2s for B-I. (F,G) *Tg(cC:gfp)* embryos were injected with morpholinos against *sp5l* and *bts1* (G), or with morpholinos against these genes, but carrying mismatches (F) (four independent experiments). (H,I) *Tg(cC:gfp)* embryos were co-injected with morpholinos against *sp5l* and *bts1*, and with *Cherry* (H) or *Sp5l* (I) mRNAs. (J-N) *Tg(cC:gfp)* embryos were treated with DMSO (J,L) or SU5402 (K,M) from the shield stage onwards and subjected to *gfp* ISH at 1s. (N) Distribution of *Tg(cC:gfp)* embryos according to the expression of *gfp*. The significance of differences was evaluated by Fisher's Exact Test: **P*<0.05; ***P*<0.02.

C activity from a loss of Fgf signalling. Together, these results demonstrate that, for *krox20* expression, Fgf signalling is mediated by *sp5l* and/or *bts1*, acting directly on element C.

Fgf signalling controls the level of enhancer C activity, but not its AP distribution

To analyse more precisely the effect of Fgf signalling on the activity of enhancer C, we interfered with Fgf signal transmission and measured the *gfp* output together with *krox20* expression along the AP axis by semi-quantitative fluorescent *in situ* hybridization (FISH; supplementary material Fig. S7). At 2s, in control embryos, *krox20* expression in r3 covers a domain four to five cells wide, with sharp anterior and posterior boundaries (Fig. 7A; *n*=9; supplementary material Fig. S7A). By contrast, the domain of activity of the wild-type enhancer C is 10-11 cells wide, displays a sharp anterior limit corresponding to the r2/r3 boundary, but progressively decreases caudally, uninterrupted by the r3/r4 boundary (Fig. 7B; *n*=10). Mutation of the Sp site results in a dramatic reduction in enhancer activity (73%; *t*-test, *P*<0.005), but the progressive AP decrease from the middle of r3 is maintained (Fig. 7C; *n*=8), as well as the activity anterior limit at the r2/3 boundary (Fig. 5H). Fitting of the points with decreasing exponentials indicates that the patterns of activity of wild-type and mutant elements C are similar and that the mutation results in a uniform decrease of activity along the AP axis (supplementary material Fig. S8A,B).

Upon SU5402 treatment, the domain of *krox20* expression is reduced to approximately two to three cells wide (*n*=6; Fig. 7D; supplementary material Fig. S7A,B). Although there is a general size reduction of the hindbrain under these conditions, this effect is of disproportionate magnitude (Fig. 7A,D; and C. Labalette, unpublished). Within this smaller *krox20*-positive domain, the level of expression remains homogenous. SU5402 treatment affects enhancer C activity differently than *krox20* itself: its level is reduced by 57% (*t*-test, *P*<0.02, *n*=10; Fig. 7B,E), and the size reduction of the domain reflects that of the hindbrain. After normalising for hindbrain size reduction (supplementary material Fig. S8C,D), the relative pattern of element C activity along the AP axis in SU5402-treated embryos and controls is comparable (supplementary material Fig. S8A,D). Therefore, as shown by two different loss-of-function

Development (2015) 142, 185-195 doi:10.1242/dev.109652

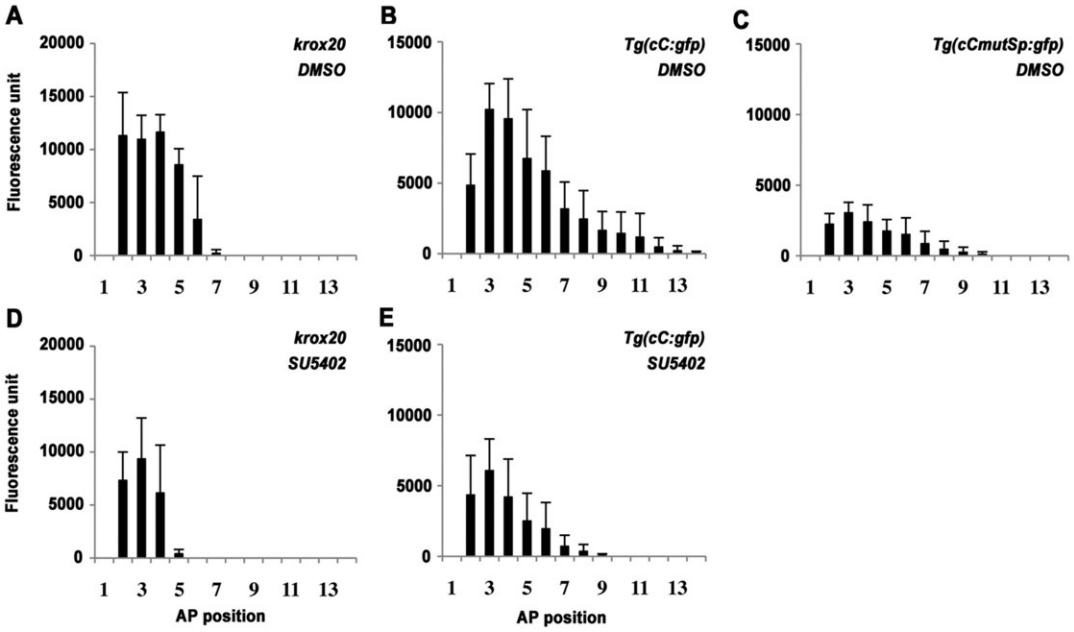

Fig. 7. Fgf signalling does not affect the relative spatial distribution of enhancer C activity. (A-E) Wild-type, *Tg(cC:gfp)* and *Tg(cCmutSp:gfp)* embryos were treated with DMSO or SU5402 from the shield stage, and subjected to FISH for *krox20* or *gfp* at 2s (see Fig. 5; supplementary material Fig. S4). The level of the fluorescent signal in each cell along the AP axis was then quantified from confocal images in ImageJ (see supplementary material Fig. S4). Each graph represents the distribution of the mean level of fluorescence at successive AP positions in at least eight embryos. Errors bars indicate s.e.m.

approaches (SU5402 treatment and mutation of the Sp site), Fgf signalling does not affect the AP domain of enhancer C activity, but rather modulates its level in a uniform manner.

We finally asked whether other components of the Fgf effector pathway showed a pattern of activity consistent with this observation. We examined the distribution of phosphorylated ERK1/2 (pERK1/2; pMapk3/pMapk1 – ZFIN database), a central mediator of the Ras/ERK pathway that is essential for Fgf control of *krox20* (Aragon and Pujades, 2009; and supplementary material Fig. S9A-C). At the stage of *krox20* activation in r3, we observe that the level of pERK1/2 plateaus over a large territory, extending rostrally into r2 and caudally up to r5 (supplementary material Fig. S9). This suggests that Fgf signalling is homogeneous over a region including r3-r4, thereby explaining why it is not involved in defining the AP limits of element C activity.

DISCUSSION

In this paper, we investigate the molecular mechanisms governing the formation of one of the hindbrain segments, rhombomere 3. The specification of this rhombomere is determined by the persistent expression of the transcription factor Krox20, which engages cells in an odd-numbered rhombomere (i.e. r3/r5) fate. We show that the delimitation of r3 is controlled by two types of inputs that act on a single *krox20* cis-acting sequence: the Hox PG1 transcription factors and their mediators, and the Fgf signalling cascade. These converging regulatory pathways use different molecular strategies to control the extent of r3. We propose a model explaining how these mechanisms can be integrated and interpreted by the *krox20* positive-feedback loop to shape *krox20* expression profile and therefore pattern the r2-r4 region.

Enhancer C integrates an incoherent feed-forward loop governed by Hox PG1 proteins

Our study has revealed that Hox PG1 factors exert an antagonistic action on *krox20* transcription via element C. *krox20* activation by Hox factors requires direct binding of Hox/Pbx/Meis complexes to element C (Wassef et al., 2008), whereas repression is indirect and involves Nlz1, which is positively regulated by Hox PG1 proteins (Figs 1-4). This constitutes an incoherent feed-forward loop converging on element C (Fig. 8A). This type of regulatory system has been shown to accelerate the response of the target gene (Mangan and Alon, 2003).

In addition, our data indicate that the balance between activation and repression is influenced by the levels of Hox PG1 proteins (Fig. 1A-D; supplementary material Figs S1,S3). This might originate from a non-linear transcriptional activation of *krox20* and *nlz1* by the Hox factors. Indeed, low levels of Hox proteins are sufficient to fully activate *krox20*, whereas higher levels are required for *nlz* activation (supplementary material Fig. S10). In the presence of high levels of Hox PG1 proteins, both *krox20* and *nlz1* are initially activated, but repression mediated by Nlz1 rapidly leads to abortive *krox20* induction. By contrast, low levels of Hox PG1 proteins can only activate *krox20*, which in turn represses Hox PG1 genes and reinforces its own expression (Fig. 8A; and Bouchoucha et al., 2013; Giudicelli et al., 2001). The network thus leads to a bifurcation, with two mutually exclusive cell fates: *krox20* on/*hoxb1* off and *krox20* off/*hoxb1* on, corresponding to r3 and r4 identities, respectively.

The interplay between Hox PG1 and Nlz factors on enhancer C is essential for positioning r3 boundaries

In prospective r3, Hox PG1 genes are transiently expressed, allowing *krox20* activation (Wassef et al., 2008). Moderate ectopic *hoxb1a* expression leads to rostral activation of enhancer C and extension of the *krox20*-positive domain to r2 (Figs 1 and 4). These observations, together with loss-of-function experiments (Figs 1 and 4), indicate that Hox PG1 proteins are limiting factors for element C activity and that they restrict the rostral extension of *krox20* expression and therefore of r3. However, as *krox20* cannot be activated anteriorly to prospective r2, additional limiting or repressing factor(s) must be involved.

Development (2015) 142, 185-195 doi:10.1242/dev.109652

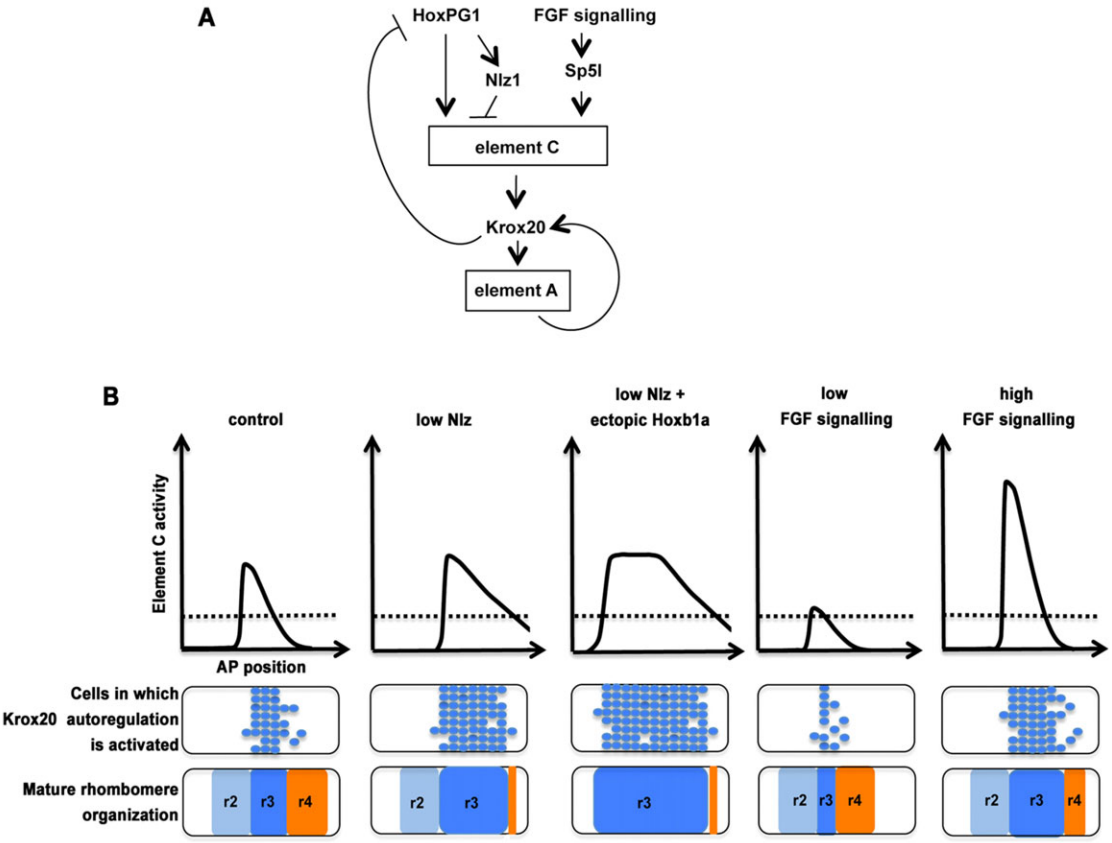

Fig. 8. A model for the determination of r3 boundaries. (A) Schematic representation of the regulatory network governing the expression of *krox20* in the r2-r4 region. Enhancer C is an initiator element, whereas enhancer A is a positive autoregulatory element. (B) The level of enhancer C activity along the AP axis, which is likely to be proportional to the initial dose of Krox20, under different, experimentally tested Nlz, Hoxb1a and Fgf signalling conditions. The activation of the autoregulatory loop according to the dose of initial Krox20 is probabilistic, and a dotted line is shown, corresponding to a 50% chance of activating the feedback loop. Activation of the feedback loop is usually irreversible, and cells in which element C activity is above the dotted line have a >50% probability of becoming r3 cells. A possible distribution of r3 cells (blue) is shown below the graphs. Maturation of rhombomere territories leads to boundary sharpening.

nlz1 is initially activated in r4 and posteriorly, and, at later stages, when *krox20* expression is already established, it extends into r3 (Runko and Sagerström, 2003), presumably initially reflecting the dynamics of Hox PG1 expression (McClintock et al., 2001). A reduction in the level of Nlz repressors results in a posterior extension of the activity of element C (Fig. 4 and Fig. 8B). This indicates that the distribution of Nlz factors is an essential determinant of the caudal limit of enhancer C activity (Fig. 8B). In prospective r3, low and/or late activation of *nlz1* is insufficient to prevent *krox20* activation by Hox PG1 factors. By contrast, in prospective r4, high/early levels of Nlz factors do not allow effective initial *krox20* expression. Therefore, the extension of the domain of activity of element C depends on the balance between activating and repressing activities of Hox PG1 factors, which is likely to reflect the dynamics of Hox PG1 expression.

In conclusion, the domain of activity of element C is delimited both rostrally and caudally by positional cues generated by Hox PG1 genes. The rostral limit reflects the anterior-most extension of Hox PG1 gene expression, and the caudal limit corresponds to the point where negative regulation exceeds positive inputs. This subsequently positions the r2/r3 and r3/r4 boundaries. Other factors are likely to be involved in regulating *krox20* in r3. Retinoic acid has been shown to repress *krox20* expression (Niederreither et al., 2000), but it might act through Hox PG1 genes (Studer et al., 1994). Hox PG2 factors are not required for *Krox20* expression in physiological conditions (Davenne et al., 1999). However, as they can activate *Krox20* in r2 (although with lower efficiency than PG1 factors) in chick (Wassef et al., 2008) and zebrafish (C. Labalette, unpublished), they might be involved in the residual activation of *Krox20* observed in *Hoxa1/Hoxb1* double mutants (Rossel and Capecchi, 1999).

Graded regulation of enhancer C activity by Fgf signalling

Fgfs activate a complex downstream cascade, involving multiple, interconnected pathways. We have assembled the Fgf-dependent molecular pathway that controls *krox20* expression in prospective r3, and have shown that signalling is mediated by Sp5l and/or Bts1, which act directly on enhancer C. In contrast to the action of Hox PG1/Nlz factors, which shape the AP pattern of element C activity by positioning its rostral and caudal limits, variations in Fgf signalling affect the level of element C activity in a uniform manner along the AP axis (Fig. 7 and Fig. 8B). This uniform effect is likely to result from a homogeneous distribution of the Fgf signal over the r3-r4 region (supplementary material Fig. S9). Consistently, general overexpression of Sp5l only increases the level of activity of enhancer C, without extending its domain (Fig. 6B,C). Hence, we propose that Fgf signalling does not provide positional cues that delimit the domain of activity of element C, but simply modulates enhancer activity like a rheostat. This effect has nevertheless important consequences on the patterning of r3, as the level of Fgf signalling determines the size of r3, by positioning the r3/r4 boundary. How graded regulation of enhancer C is translated into

Development (2015) 142, 185-195 doi:10.1242/dev.109652

patterning information is a crucial issue, which is discussed below. Finally, it has also been shown that Sp5 factors mediate the downstream response to Wnt signalling involved in global AP hindbrain patterning (Weidinger et al., 2005). Wnt and Fgf signalling pathways might therefore cooperate via Sp5 factors to delimit r3.

A model for the patterning of the r2-r4 region

We have identified two important pathways converging on element C (Fig. 8A). First, Hox PG1 activators and Nlz repressors provide positional cues defining the AP limits of its domain of activity; and second, Fgf signalling uniformly modulates this activity. However, modulation of enhancer activity cannot directly translate into boundary positions. These two pathways must be integrated with a third regulatory component, the positive-feedback loop. *Krox20* is subject to positive autoregulation, governed by another previously identified cis-acting sequence, element A (Chomette et al., 2006; Giudicelli et al., 2001). This feedback loop underpins a bistable switch that turns a transient input into cell fate commitment for odd- or even-numbered rhombomere identities (Bouchoucha et al., 2013). Due to the stochastic nature of the molecular mechanisms involved in the loop, each cell has a defined probability of activating the autoregulatory loop and stably expressing *krox20*, according to the initial dose of Krox20. This allows the definition of a dose, above which a cell has a more than 50% probability of activating the loop.

Taking autoregulation into account, we propose a model for the patterning of the r2-r4 region that relies on the following steps (Fig. 8B): first, a pattern of activity of element C along the AP axis is established by Hox PG1 factors through both positive and Nlz-dependant negative actions, resulting in a sharp anterior surge and an exponential-like decrease posteriorly (Fig. 7; and supplementary material Fig. S8). Second, a uniform modulation of this pattern by Fgf signalling determines the initial dose of Krox20 in each cell according to its AP position (Fig. 8B). The dose curve intersects the line for triggering autoregulation with a 50% chance at two positions. Third, the bistable switch leads to permanent activation of *krox20* according to the initial dose of Krox20 and to its probabilistic rules. As the initial AP distribution of Krox20 dose crosses the 50% line, a fuzzy boundary is established between *krox20*-positive and -negative domains and is subsequently refined by additional mechanisms (Cooke et al., 2005; Mellitzer et al., 1999; Zhang et al., 2012).

This model accounts for the displacements of r3 boundaries following manipulation of Hox PG1 or Nlz expression, or Fgf signalling (Fig. 8B). In the cases of Hox PG1 and Nlz, variations in their distributions lead to modifications in the AP domain of element C activity (Fig. 8B). In the case of Fgf signalling, variations result in uniform modifications in the level of element C activity. The AP distribution of the activity is asymmetrical, with a sharp anterior transition and a gently decreasing slope posteriorly (Fig. 8B). Thus, uniform modification does not significantly affect the position of its anterior intersection with the threshold line, whereas it does lead to a significant displacement of the posterior intersection. This translates into the position of the r2/r3 boundary being relatively insensitive to changes in Fgf signalling, whereas that of the r3/r4 boundary is very sensitive (Fig. 8B). In this context, Fgfs perform a morphogenetic role, but do not act as classical morphogens distributed in gradients. They shape tissue identity by uniformly modulating a pre-existing response pattern of a cis-acting enhancer element, coupled with a positive-feedback loop that drives a bistable cell fate choice.

MATERIALS AND METHODS

Zebrafish lines and injections

All animal experimentation was performed according to French and European regulations (French agreement: Ce5/2012/138). Embryos were treated with 60 µM SU5402 (Calbiochem) as described (Walshe et al., 2002). For mRNA injection, *hoxb1a* capped-sense RNA was generated with a plasmid obtained from Victoria Prince (University of Chicago, USA), using the mMESSAGE mMACHINE kit (Ambion). At the one-cell stage, 15-150 pg of mRNA were injected. For morpholino injections, morpholinos (Gene Tools) were diluted in Danieau buffer and 2 pmol were injected at the one- to four-cell stage. Most morpholinos were described previously: *hoxb1a* and *hoxb1b* (McClintock et al., 2002), *nlz1* and *nlz2* (Hoyle et al., 2004), *spry4* (Furthauer et al., 2001, 2004), *sp5l* (Labalette et al., 2011; Weidinger et al., 2005), *bts1* (Tallafuss et al., 2001) and control morpholino (Labalette et al., 2011). Specific control morpholinos for the *sp5l*/*bts1* morpholinos were obtained by the introduction of five mismatches in each morpholino. Transgenic lines were obtained from embryos injected at the one-cell stage with pTol2 constructs together with 50 pg of *tol2* transposase mRNA (Kawakami et al., 2004). The phenotypes observed in this study are very reproducible: 100% of the embryos show the phenotype in case of heat shocks and more than 80% with the different morpholinos. The numbers indicated in the text correspond to the affected embryos. All experiments correspond to at least two independent injections. When more independent injections were taken into account, this is indicated in the figure legends.

In situ hybridization (ISH), immunostaining and fluorescence quantification

Single and double whole-mount ISHs were performed as described (Hauptmann and Gerster, 1994). To generate the *nlz1* probe, a fragment from pCS2-Nlz1 (Runko and Sagerström, 2003) was subcloned into the pCRII-TOPO2.1 vector. To generate the *gfp* probe, the coding region (positions 1 to 753) was subcloned into pBluescript. The other probes used were described previously: zebrafish *krox20* (Oxtoby and Jowett, 1993), *ntl* (Schulte-Merker et al., 1994), *pax2.1* (Krauss et al., 1991), *mafba* (Moens et al., 1998) and *hoxb1a* (Prince et al., 1998). Immunostaining was performed with a polyclonal rabbit antibody against pERK1/2 (Cell Signaling, #9101; 1/200 dilution) and a monoclonal rat antibody against GFP (Nacalai Tesque, #04404-84; 1/200 dilution), and with Alexa 488- and Alexa 594-conjugated secondary antibodies (Jackson ImmunoResearch, anti rabbit: #711-545-152; 1/400 dilution; anti rat: #712-585-153; 1/400 dilution). For FISH, Fast Red tablets (Roche) were used as substrates for the reaction. For fluorescence quantification, flat-mounted embryos were imaged on a Leica TCS SP5 confocal microscope. Images were acquired in 16-bit format to allow the estimation of fluorescence with ImageJ (NIH). Fluorescence levels were quantified in single nuclei for pERK1/2 immunostaining or in single cells for *krox20* or *gfp* ISH. A disk of the same area was defined within each nucleus or cell to perform measurements. All cells along an AP axis through the middle of the left and right sides were measured, and the two sides were averaged (see supplementary material Fig. S7).

Constructs

To obtain the *pTol2-hsp:hoxb1a* construct, *pCS2-hoxb1a-Myc* (McClintock et al., 2001) was digested by *Hin*dIII, blunt-ended and digested with *Not*I. The *hoxb1a-Myc* fragment was cloned together with *Sma*I- and *Xho*I-digested pBluescript-hsp (Halloran et al, 2000) into the pTol2 vector (Kawakami et al., 2004) digested with *Not*I and *Xho*I. The *Tg(cC:gfp)* line was generated by injection of the *pTol2-cC:gfp* construct, obtained by cloning of a 1042-bp fragment containing chick element C (Wassef et al., 2008) into the pTol2-GFP vector. The element C DNA fragment was obtained by PCR amplification with the following oligonucleotide primers: 5′-TACGAATTCTGAGTACTGAATGTGCAGAGTTTGGC-3′ and 5′-TACGAGCTCACCCAAGACAGTCCCGCAGT-3′. To mutate the Sp-binding site (*pTol2-cCmutSp:gfp*), a mutation was introduced using PCR-mediated mutagenesis with the high fidelity Phusion Taq polymerase (Finnzyme), replacing the sequence GTGGGTGGA with GGGGGGGGA. To generate an inducible Sp5l expression vector (*pTol2-hsp:sp5l-HA*), a

*Not*I-*Xho*I *Sp5l-HA* DNA fragment from pCS2-Sp5l-HA (Sun et al., 2006) was subcloned into the pTol2 vector (Stedman et al., 2009).

Protein extracts and gel retardation assays

For preparation of protein extracts containing SP5, the mouse SP5-coding sequence was cloned into the pAdRSVSp vector (Giudicelli et al., 2003) together with an HA epitope-coding sequence just before the stop codon. The expression plasmid was transfected into COS-7 cells using Lipofectamine 2000 transfection reagent (Invitrogen). Cell lysates were prepared as previously described (Wassef et al., 2008). Gel retardation assays were performed with SP5-HA protein extracts as previously described (Chomette et al., 2006), except for the composition of the incubation buffer (4% glycerol, 1 mM $MgCl_2$, 0.5 mM EDTA, 0.5 mM DTT, 50 mM NaCl, 10 mM Tris pH 7.5; 0.2 mM $ZnCl_2$). The same 21-bp double-stranded oligonucleotide was used as probe and competitor, and was obtained by annealing the following oligonucleotides: sense, 5′-AGGGT-TGTTCCACCCACCCAT-3′; antisense, 5′-AGATGGGTGGGTGGAAC-AACC-3′. The mutant competitor carried the following modifications (underlined) in the Sp-binding site: AGG-GTTGTTCCCCCCCCCCAT. Anti-Flag (Sigma, #F3165; 1/10 dilution) and anti-HA (Roche, #1186742300; 1/10 dilution) antibodies were used for the supershift experiments.

Double *in situ* hybridization/immunostaining

For double labelling, ISH was performed using the Fast Red substrate (Roche), and followed by immunostaining using a rabbit polyclonal antibody against phospho-Histone H3 (Upstate, #06-57032219; 1/400 dilution) and a mouse monoclonal antibody directed against the Myc-tag (clone 9E10, Sigma; #M5546; 1/200 dilution). These were revealed using Alexa 488-coupled anti-rabbit and Cy5-coupled anti-mouse goat antibodies (Jackson, anti rabbit: #711-545-152; 1/400 dilution; anti mouse: #115-175-146; 1/400 dilution).

Acknowledgements

We are grateful to V. Prince for providing us with the pCS2-hoxb1a plasmid and to C. Sagerstrom for the pCS2-nlz1 plasmid.

Competing interests

The authors declare no competing financial interests.

Author contributions

C.L., M.A.W., Y.X.B., J.L.M., P.C. and P.G.-H. conceived and designed the experiments. C.L., M.A.W., C.D.-T.D., Y.X.B., J.L.M. and P.G.-H. performed the experiments. C.L., M.A.W., C.D.-T.D., Y.X.B., J.L.M., P.C. and P.G.-H. analysed the data. C.L., Y.X.B., P.C. and P.G.-H. wrote the paper.

Funding

This work was funded by grants from Ministère de l'Enseignement Supérieur et de la Recherche, Institut National de la Santé et de la Recherche Médicale, Centre National de la Recherche Scientifique and Agence Nationale de la Recherche (ANR). It has received support under the program 'Investissements d'Avenir' launched by the French Government and implemented by the ANR [ANR-10-LABX-54 MEMOLIFE and ANR-11-IDEX-0001-02 PSL* Research University]. C.L. was supported by grants from Fondation de la Recherche Médicale [SPE20060406807], Neuropole-Ile-de-France [IF 09-2095/R] and [ANR R08076JJ].

Supplementary material

Supplementary material available online at
http://dev.biologists.org/lookup/suppl/doi:10.1242/dev.109652/-/DC1

References

Aragon, F. and Pujades, C. (2009). FGF signaling controls caudal hindbrain specification through Ras-ERK1/2 pathway. *BMC Dev. Biol.* **9**, 61.
Barrow, J. R., Stadler, H. S. and Capecchi, M. R. (2000). Roles of Hoxa1 and Hoxa2 in patterning the early hindbrain of the mouse. *Development* **127**, 933-944.
Berg, J. M. (1992). Sp1 and the subfamily of zinc finger proteins with guanine-rich binding sites. *Proc. Natl. Acad. Sci. USA* **89**, 11109-11110.
Bouchoucha, Y. X., Reingruber, J., Labalette, C., Wassef, M. A., Thierion, E., Desmarquet-Trin Dinh, C., Holcman, D., Gilardi-Hebenstreit, P. and Charnay, P. (2013). Dissection of a Krox20 positive feedback loop driving cell fate choices in hindbrain patterning. *Mol. Syst. Biol.* **9**, 690.
Chomette, D., Frain, M., Cereghini, S., Charnay, P. and Ghislain, J. (2006). Krox20 hindbrain cis-regulatory landscape: interplay between multiple long-range initiation and autoregulatory elements. *Development* **133**, 1253-1262.
Cooke, J. E., Kemp, H. A. and Moens, C. B. (2005). EphA4 is required for cell adhesion and rhombomere-boundary formation in the zebrafish. *Curr. Biol.* **15**, 536-542.
Davenne, M., Maconochie, M. K., Neun, R., Pattyn, A., Chambon, P., Krumlauf, A. and Rijli, F. M. (1999). Hoxa2 and Hoxb2 control dorsoventral patterns of neuronal development in the rostral hindbrain. *Neuron* **22**, 677-691.
de Laat, W. and Duboule, D. (2013). Topology of mammalian developmental enhancers and their regulatory landscapes. *Nature* **502**, 499-506.
Furthauer, M., Reifers, F., Brand, M., Thisse, B. and Thisse, C. (2001). sprouty4 acts in vivo as a feedback-induced antagonist of FGF signaling in zebrafish. *Development* **128**, 2175-2186.
Fürthauer, M., Van Celst, J., Thisse, C. and Thisse, B. (2004). Fgf signalling controls the dorsoventral patterning of the zebrafish embryo. *Development* **131**, 2853-2864.
Garcia-Dominguez, M., Gilardi-Hebenstreit, P. and Charnay, P. (2006). PIASxbeta acts as an activator of Hoxb1 and is antagonized by Krox20 during hindbrain segmentation. *EMBO J.* **25**, 2432-2442.
Gavalas, A., Studer, M., Lumsden, A., Rijli, F. M., Krumlauf, R. and Chambon, P. (1998). Hoxa1 and Hoxb1 synergize in patterning the hindbrain, cranial nerves and second pharyngeal arch. *Development* **125**, 1123-1136.
Gilland, E. and Baker, R. (1993). Conservation of neuroepithelial and mesodermal segments in the embryonic vertebrate head. *Acta Anat. (Basel)* **148**, 110-123.
Giudicelli, F., Taillebourg, E., Charnay, P. and Gilardi-Hebenstreit, P. (2001). Krox-20 patterns the hindbrain through both cell-autonomous and non cell-autonomous mechanisms. *Genes Dev.* **15**, 567-580.
Halloran, M. C., Sato-Maeda, M., Warren, J. T., Su, F., Lele, Z., Krone, P. H., Kuwada, J. Y. and Shoji, W. (2000). Laser-induced gene expression in specific cells of transgenic zebrafish. *Development* **127**, 1953-1960.
Harrison, S. M., Houzelstein, D., Dunwoodie, S. L. and Beddington, R. S. P. (2000). Sp5, a new member of the Sp1 family, is dynamically expressed during development and genetically interacts with Brachyury. *Dev. Biol.* **227**, 358-372.
Hauptmann, G. and Gerster, T. (1994). Two-color whole-mount in situ hybridization to vertebrate and Drosophila embryos. *Trends Genet.* **10**, 266.
Helmbacher, F., Pujades, C., Desmarquet, C., Frain, M., Rijli, F. M., Chambon, P. and Charnay, P. (1998). Hoxa1 and Krox-20 synergize to control the development of rhombomere 3. *Development* **125**, 4739-4748.
Hoyle, J., Tang, Y. P., Wiellette, E. L., Wardle, F. C. and Sive, H. (2004). nlz gene family is required for hindbrain patterning in the zebrafish. *Dev. Dyn.* **229**, 835-846.
Kawakami, K., Takeda, H., Kawakami, N., Kobayashi, M., Matsuda, N. and Mishina, M. (2004). A transposon-mediated gene trap approach identifies developmentally regulated genes in zebrafish. *Dev. Cell* **7**, 133-144.
Kicheva, A., Cohen, M. and Briscoe, J. (2012). Developmental pattern formation: insights from physics and biology. *Science* **338**, 210-212.
Krauss, S., Johansen, T., Korzh, V. and Fjose, A. (1991). Expression of the zebrafish paired box gene pax[zf-b] during early neurogenesis. *Development* **113**, 1193-1206.
Labalette, C., Bouchoucha, Y. X., Wassef, M. A., Gongal, P. A., Le Men, J., Becker, T., Gilardi-Hebenstreit, P. and Charnay, P. (2011). Hindbrain patterning requires fine-tuning of early krox20 transcription by Sprouty 4. *Development* **138**, 317-326.
Lander, A. D. (2011). Pattern, growth, and control. *Cell* **144**, 955-969.
Lumsden, A. (1990). The cellular basis of segmentation in the developing hindbrain. *Trends Neurosci.* **13**, 329-335.
Lumsden, A. and Keynes, R. (1989). Segmental patterns of neuronal development in the chick hindbrain. *Nature* **337**, 424-428.
Lumsden, A. and Krumlauf, R. (1996). Patterning the vertebrate neuraxis. *Science* **274**, 1109-1115.
Makki, N. and Capecchi, M. R. (2010). Hoxa1 lineage tracing indicates a direct role for Hoxa1 in the development of the inner ear, the heart, and the third rhombomere. *Dev. Biol.* **341**, 499-509.
Mangan, S. and Alon, U. (2003). Structure and function of the feed-forward loop network motif. *Proc. Natl. Acad. Sci. USA* **100**, 11980-11985.
Marin, F. and Charnay, P. (2000). Hindbrain patterning: FGFs regulate Krox20 and mafB/kr expression in the otic/preotic region. *Development* **127**, 4925-4935.
Maves, L., Jackman, W. and Kimmel, C. B. (2002). FGF3 and FGF8 mediate a rhombomere 4 signaling activity in the zebrafish hindbrain. *Development* **129**, 3825-3837.
McClintock, J. M., Carlson, R., Mann, D. M. and Prince, V. E. (2001). Consequences of Hox gene duplication in the vertebrates: an investigation of the zebrafish Hox paralogue group 1 genes. *Development* **128**, 2471-2484.
McClintock, J. M., Kheirbek, M. A. and Prince, V. E. (2002). Knockdown of duplicated zebrafish hoxb1 genes reveals distinct roles in hindbrain patterning and a novel mechanism of duplicate gene retention. *Development* **129**, 2339-2354.
McKay, I. J., Lewis, J. and Lumsden, A. (1996). The role of FGF-3 in early inner ear development: an analysis in normal and kreisler mutant mice. *Dev. Biol.* **174**, 370-378.
McNulty, C. L., Peres, J. N., Bardine, N., van den Akker, W. M. R. and Durston, A. J. (2005). Knockdown of the complete Hox paralogous group 1 leads to dramatic hindbrain and neural crest defects. *Development* **132**, 2861-2871.

Meinhardt, H. (2009). Models for the generation and interpretation of gradients. *Cold Spring Harb. Perspect. Biol.* **1**, a001362.
Mellitzer, G., Xu, Q. and Wilkinson, D. G. (1999). Eph receptors and ephrins restrict cell intermingling and communication. *Nature* **400**, 77-81.
Moens, C. B. and Prince, V. E. (2002). Constructing the hindbrain: insights from the zebrafish. *Dev. Dyn.* **224**, 1-17.
Moens, C. B., Cordes, S. P., Giorgianni, M. W., Barsh, G. S. and Kimmel, C. B. (1998). Equivalence in the genetic control of hindbrain segmentation in fish and mouse. *Development* **125**, 381-391.
Monk, K. R., Naylor, S. G., Glenn, T. D., Mercurio, S., Perlin, J. R., Dominguez, C., Moens, C. B. and Talbot, W. S. (2009). A G protein-coupled receptor is essential for Schwann cells to initiate myelination. *Science* **325**, 1402-1405.
Nakamura, M., Choe, S.-K., Runko, A. P., Gardner, P. D. and Sagerström, C. G. (2008). Nlz1/Znf703 acts as a repressor of transcription. *BMC Dev. Biol.* **8**, 108.
Niederreither, K., Vermot, J., Schuhbaur, B., Chambon, P. and Dollé, P. (2000). Retinoic acid synthesis and hindbrain patterning in the mouse embryo. *Development* **127**, 75-85.
Oxtoby, E. and Jowett, T. (1993). Cloning of the zebrafish krox-20 gene (krx-20) and its expression during hindbrain development. *Nucleic Acids Res.* **21**, 1087-1095.
Prince, V. E., Moens, C. B., Kimmel, C. B. and Ho, R. K. (1998). Zebrafish hox genes: expression in the hindbrain region of wild-type and mutants of the segmentation gene, valentino. *Development* **125**, 393-406.
Rossel, M. and Capecchi, M. R. (1999). Mice mutant for both Hoxa1 and Hoxb1 show extensive remodeling of the hindbrain and defects in craniofacial development. *Development* **126**, 5027-5040.
Runko, A. P. and Sagerström, C. G. (2003). Nlz belongs to a family of zinc-finger-containing repressors and controls segmental gene expression in the zebrafish hindbrain. *Dev. Biol.* **262**, 254-267.
Runko, A. P. and Sagerström, C. G. (2004). Isolation of nlz2 and characterization of essential domains in Nlz family proteins. *J. Biol. Chem.* **279**, 11917-11925.
Schneider-Maunoury, S., Topilko, P., Seitanidou, T., Levi, G., Cohen-Tannoudji, M., Pournin, S., Babinet, C. and Charnay, P. (1993). Disruption of Krox-20 results in alteration of rhombomeres 3 and 5 in the developing hindbrain. *Cell* **75**, 1199-1214.
Schneider-Maunoury, S., Seitanidou, T., Charnay, P. and Lumsden, A. (1997). Segmental and neuronal architecture of the hindbrain of Krox-20 mouse mutants. *Development* **124**, 1215-1226.
Schulte-Merker, S., Hammerschmidt, M., Beuchle, D., Cho, K. W., De Robertis, E. M. and Nüsslein-Volhard, C. (1994). Expression of zebrafish goosecoid and no tail gene products in wild-type and mutant no tail embryos. *Development* **120**, 843-852.
Shen, Y., Yue, F., McCleary, D. F., Ye, Z., Edsall, L., Kuan, S., Wagner, U., Dixon, J., Lee, L., Lobanenkov, V. V. et al. (2012). A map of the cis-regulatory sequences in the mouse genome. *Nature* **488**, 116-120.
Spitz, F. and Furlong, E. E. M. (2012). Transcription factors: from enhancer binding to developmental control. *Nat. Rev. Genet.* **13**, 613-626.
Stedman, A., Lecaudey, V., Havis, E., Anselme, I., Wassef, M., Gilardi-Hebenstreit, P. and Schneider-Maunoury, S. (2009). A functional interaction between Irx and Meis patterns the anterior hindbrain and activates krox20 expression in rhombomere 3. *Dev. Biol.* **327**, 566-577.
Studer, M., Pöpperl, H., Marshall, H., Kuroiwa, A. and Krumlauf, R. (1994). Role of a conserved retinoic acid response element in rhombomere restriction of Hoxb-1. *Science* **265**, 1728-1732.
Sun, Z., Zhao, J., Zhang, Y. and Meng, A. (2006). Sp5l is a mediator of Fgf signals in anteroposterior patterning of the neuroectoderm in zebrafish embryo. *Dev. Dyn.* **235**, 2999-3006.
Swiatek, P. J. and Gridley, T. (1993). Perinatal lethality and defects in hindbrain development in mice homozygous for a targeted mutation of the zinc finger gene Krox20. *Genes Dev.* **7**, 2071-2084.
Tallafuss, A., Wilm, T. P., Crozatier, M., Pfeffer, P., Wassef, M. and Bally-Cuif, L. (2001). The zebrafish buttonhead-like factor Bts1 is an early regulator of pax2.1 expression during mid-hindbrain development. *Development* **128**, 4021-4034.
Tümpel, S., Wiedemann, L. M. and Krumlauf, R. (2009). Hox genes and segmentation of the vertebrate hindbrain. *Curr. Top. Dev. Biol.* **88**, 103-137.
Voiculescu, O., Taillebourg, E., Pujades, C., Kress, C., Buart, S., Charnay, P. and Schneider-Maunoury, S. (2001). Hindbrain patterning: Krox20 couples segmentation and specification of regional identity. *Development* **128**, 4967-4978.
Walshe, J., Maroon, H., McGonnell, I. M., Dickson, C. and Mason, I. (2002). Establishment of hindbrain segmental identity requires signaling by FGF3 and FGF8. *Curr. Biol.* **12**, 1117-1123.
Wassef, M. A., Chomette, D., Pouilhe, M., Stedman, A., Havis, E., Desmarquet-Trin Dinh, C., Schneider-Maunoury, S., Gilardi-Hebenstreit, P., Charnay, P. and Ghislain, J. (2008). Rostral hindbrain patterning involves the direct activation of a Krox20 transcriptional enhancer by Hox/Pbx and Meis factors. *Development* **135**, 3369-3378.
Weidinger, G., Thorpe, C. J., Wuennenberg-Stapleton, K., Ngai, J. and Moon, R. T. (2005). The Sp1-related transcription factors sp5 and sp5-like act downstream of Wnt/beta-catenin signaling in mesoderm and neuroectoderm patterning. *Curr. Biol.* **15**, 489-500.
Wiellette, E. L. and Sive, H. (2003). vhnf1 and Fgf signals synergize to specify rhombomere identity in the zebrafish hindbrain. *Development* **130**, 3821-3829.
Zhang, L., Radtke, K., Zheng, L., Cai, A. Q., Schilling, T. F. and Nie, Q. (2012). Noise drives sharpening of gene expression boundaries in the zebrafish hindbrain. *Mol. Syst. Biol.* **8**, 613.

SUPPLEMENTARY FIGURES

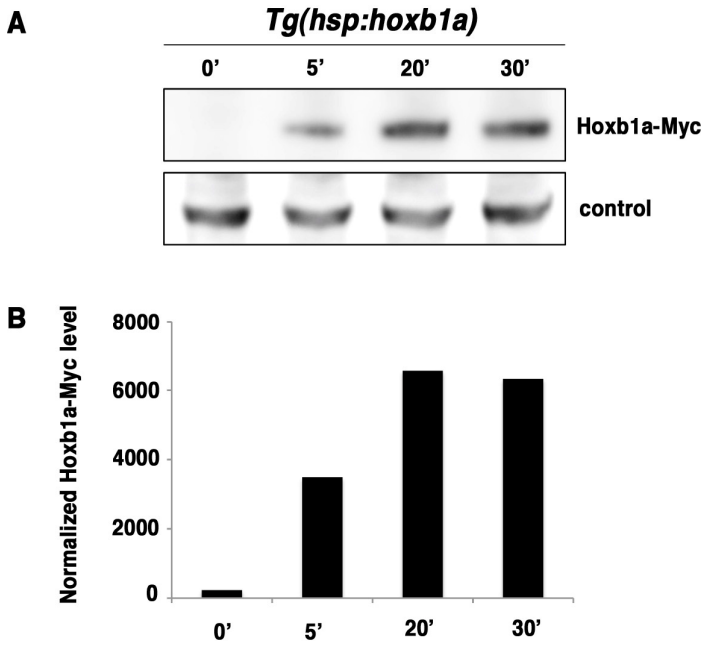

Figure S1. Dependence of the level of exogenous Hoxb1a on the length of the heat shock. (A) *Tg(hsp:hoxb1a-myc)* embryos were either not heat-shocked or heat-shocked for increasing lengths of time as indicated at 95% epiboly and collected one hour after heat shock. Pools of embryos were analysed by western blotting using an antibody directed against the Myc tag. A non-specific band corresponding to a protein not affected by the heat shock was used to normalize the amount of loaded material. (B) Quantification of the data presented in (A) using the ImageQuant software.

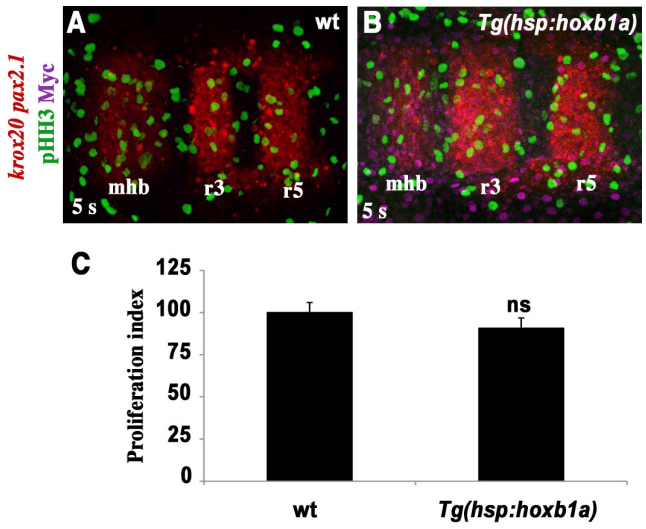

Figure S2. Cell proliferation in r3 is not affected by *hoxb1a* overexpression. (A,B) Wild-type (wt) and *Tg(hsp:hoxb1a-Myc)* embryos were heat-shocked for 5 min at 95% epiboly and collected at 5s. They were subjected to fluorescent in situ hybridization with a *krox20* probe (red), followed by double immunostaining using anti-phospho-Histone H3 (pHH3, green), a marker of mitosis, and anti-Myc-tag (magenta) antibodies. Embryos were flat-mounted with the anterior towards the left. Each figure shows merging of *z*-projections of confocal sections. (C) Normalized proliferation indexes corresponding to the mean ratio of the number of pHH3-positive cells within the rostral *krox20*-positive domain divided by the area of this domain, normalized by the mean ratio obtained with wild type embryos. No significant difference between wild type and *Tg(hsp:hoxb1a-Myc)* embryos was detected by *t*-test, $P>0.05$. Errors bars indicate s.e.m. mhb, mid-hindbrain boundary.

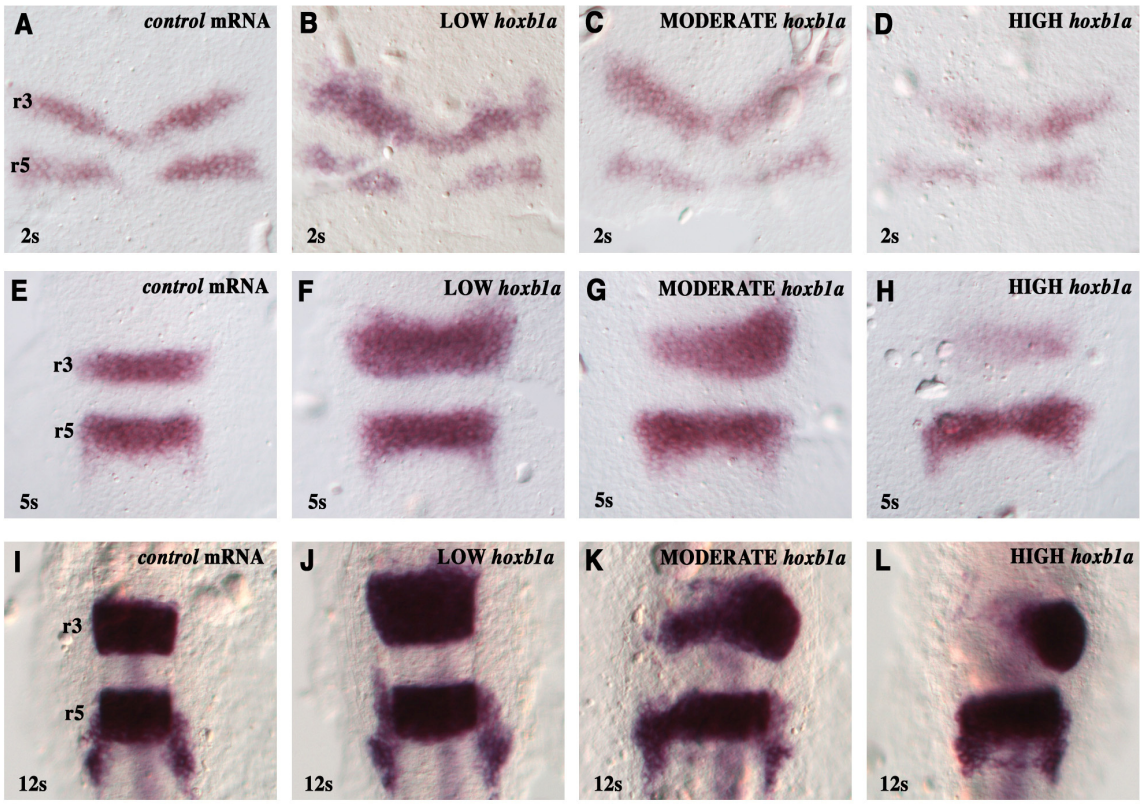

Figure S3. Dose-dependent effect of Hoxb1a on *krox20* expression. (A-L) Wild-type embryos were injected with control mRNA (*cherry-h2b)* or increasing amounts of *hoxb1a* mRNA (5, 20 and 50 ng/µl, respectively) as indicated. Embryos were collected at 2s, 5s or 12s as indicated and subjected to in situ hybridization with a *krox20* probe. The non-uniform effects of *hoxb1a* mRNA injection on *krox20* expression are due to unequal distribution of the RNA, in particular across the midline, as shown by lineage tracing analysis (Labalette, unpublished).

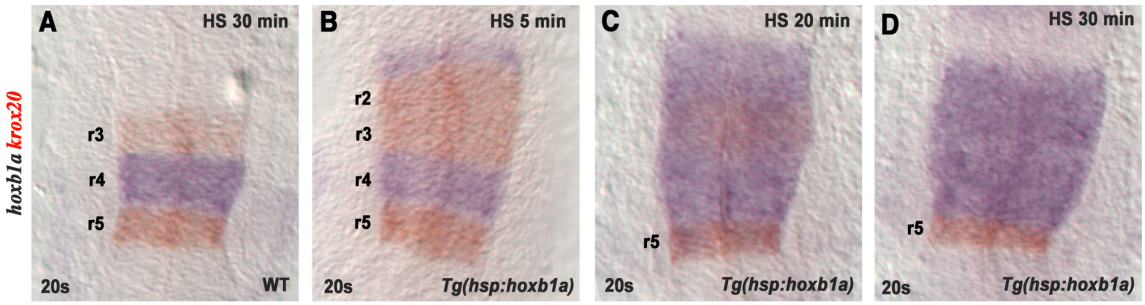

Figure S4. Ectopic Hoxb1a affects endogenous *hoxb1a* expression. Wild type (WT) and *Tg(hsp:hoxb1a)* embryos were heat-shocked for 5 (B), 20 (C) or 30 minutes (A,D) at 100% epiboly, collected at 20s and subjected to in situ hybridization for *krox20* (orange) and endogenous *hoxb1a* (purple, the probe specifically recognizes the endogenous mRNA). Embryos were flat-mounted with the anterior towards the top. At low doses of exogenous Hoxb1a, endogenous *hoxb1a* is activated anteriorly, presumably in a part of r1 (probably due to autoregulation). At higher levels, endogenous *hoxb1a* is activated over the entire r1-r4 region, reflecting loss of *krox20* expression and subsequent release of *hoxb1a* repression by Krox20. These results indicate that modifications in gene expression are not limited to *krox20*, but affect genes normally activated by Hoxb1a and repressed by Krox20.

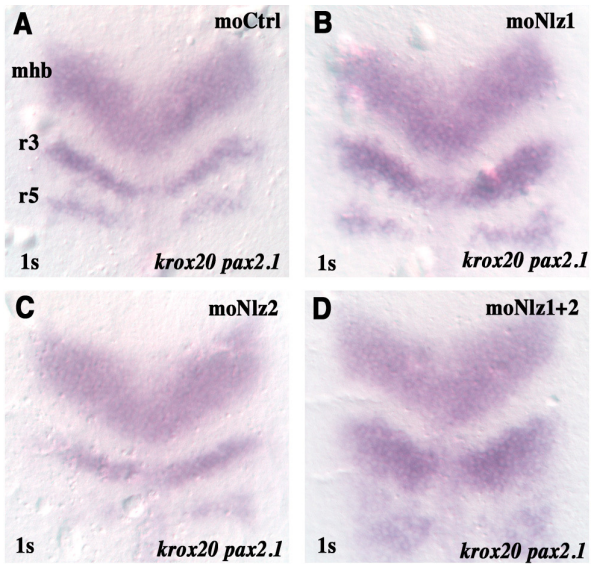

Figure S5. Nlz1 is the major actor of *krox20* repression. Wild-type embryos were injected with a control morpholino (moCtrl) or with morpholinos for *nlz1* (moNlz1), *nlz2* (moNlz2) or both (moNlz1+2), collected at 1 s and subjected to in situ hybridization with *krox20* and *pax2.1* probes (three independent experiments).

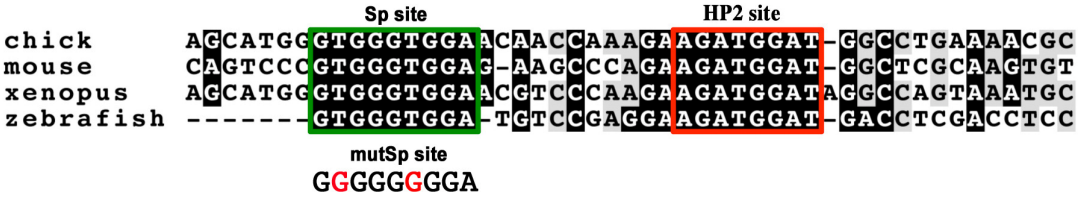

Figure S6. Alignment of vertebrate element C nucleotide sequences showing the conserved putative Sp site (green box) in the vicinity of a Hox/Pbx binding site (HP2, red box). The nucleotides modified in the mutant version of the Sp site (mutSp) are indicated in red underneath.

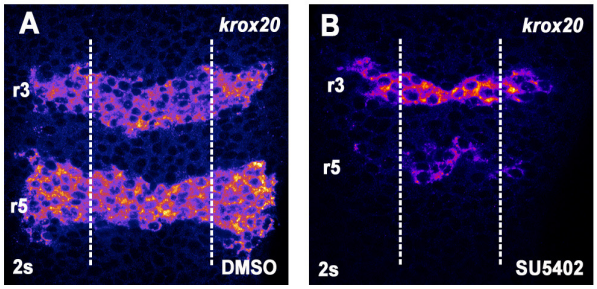

Figure S7. Analysis of *krox20* mRNA distribution using semi-quantitative, fluorescent *in situ* hybridization. (A,B) The analysis was performed on 2 s wild-type embryos, treated with DMSO or SU5402, as indicated. Embryos were flat-mounted with anterior towards the top. The dashed lines in the middle of each embryo side indicate the two AP lines along which fluorescence was measured in each cell.

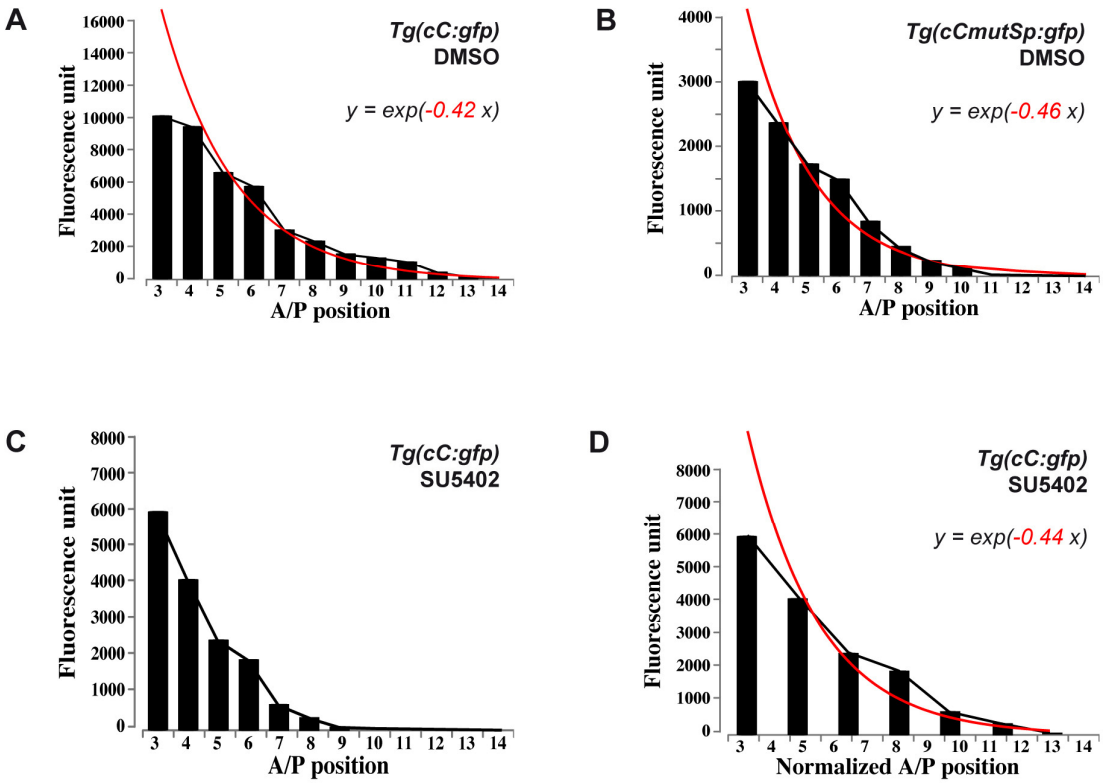

Figure S8. Quantitative analysis of element C activity profile upon variations in FGF signalling. (A-C) The profiles shown in Fig. 7B-E (black bars) are represented after normalization along the y axis, omitting the first point (point 2 in Fig. 7). (A,B) The profiles were fitted with decreasing exponentials (red curves) using the Matlab software and the equation of the best-fitting curve is shown. (D) The profile shown in C was first normalized along the *x*-axis to take into account the reduction in size of the hindbrain following SU5402 treatment (38% reduction in the length of the MHB-r6 region, data not shown) and then fitted with a decreasing exponential (red curve). Close exponential factors are found for the different curves, indicating that the normalized profiles are quantitatively similar.

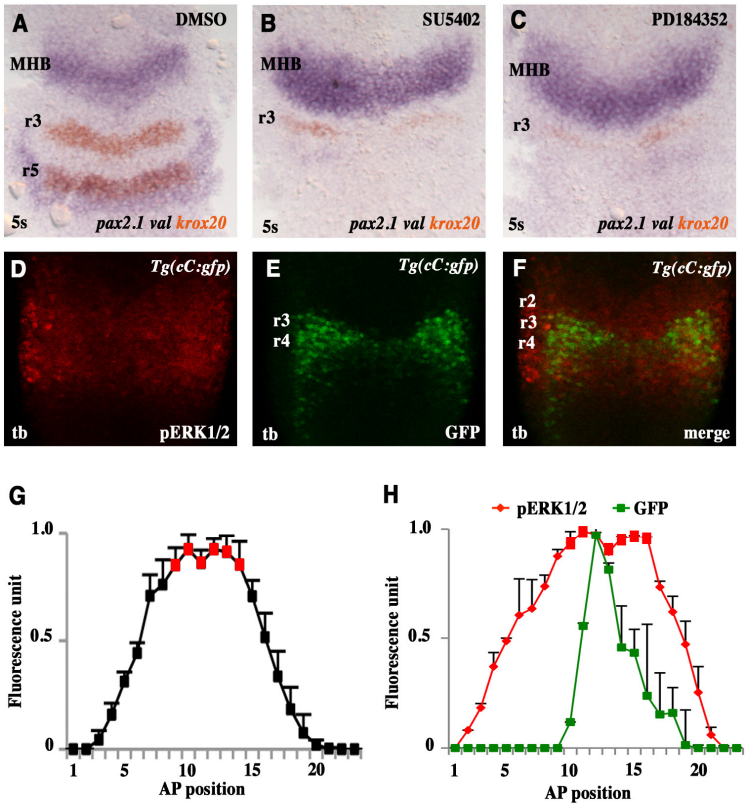

Figure S9. FGF signalling is homogeneous over a region including r3. (A-C) Embryos were treated as indicated with DMSO, SU5402 or the MEK inhibitor, PD184352, from shield to 90% epiboly, allowed to develop to 5s and subjected to *pax2.1* (purple), *krox20* (orange) and *val* (purple) in situ hybridization. (D-F) Tailbud *Tg(cC:gfp)* embryo analysed by double immunohistochemistry for pERK1/2 (red, D) and GFP (green, E). The merge is presented in (F). The positions of prospective rhombomeres are deduced from the GFP pattern. (G) Quantification of the levels of the phosphorylated forms of ERK1/2 (pERK1/2), estimated by fluorescent immunohistochemistry at 100% epiboly, along the AP axis. Measures represent the average of seven embryos. (H) Quantifications of the levels of pERK1/2 (red) and GFP (green) fluorescence at tail bud stage along the AP axis in the embryo shown in D-F. Measures represent the average of both sides of the embryos. In G,H, the red squares indicate the positions where the pERK1/2 signal differs by less than 5% from the mean of the plateau. Errors bars indicate s.e.m.

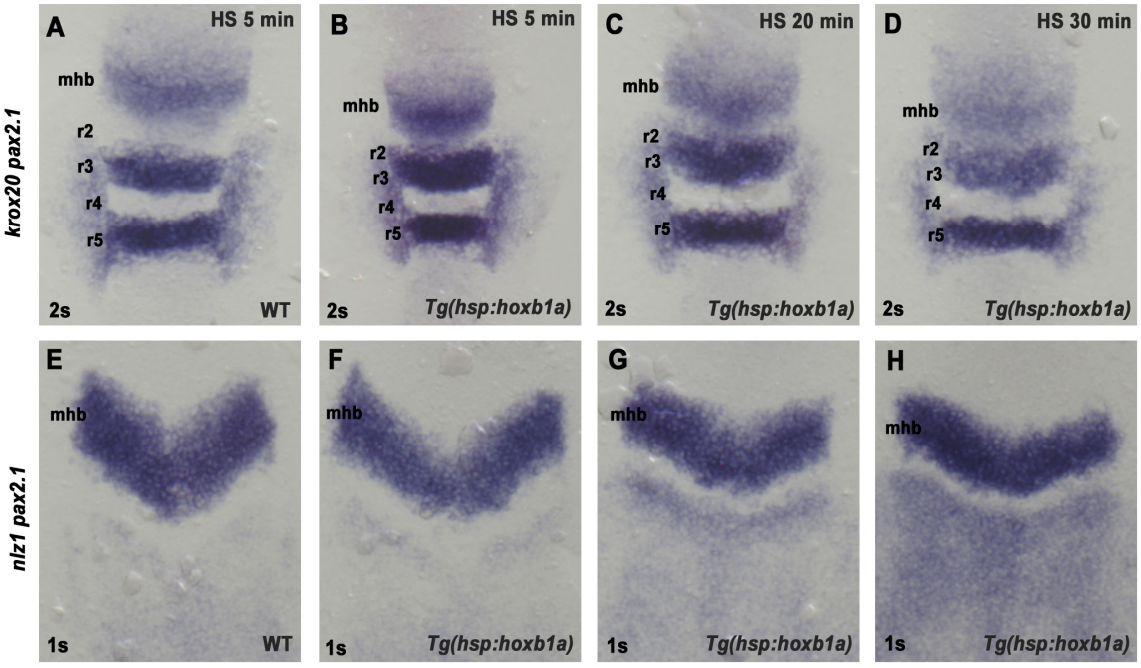

Figure S10. Different thresholds of activation by Hoxb1a for *krox20* and *nlz1*. Wild-type (WT) and *Tg(hsp:hoxb1a)* embryos were heat-shocked for 5 (A,B,E,F), 20 (C,G) or 30 min (D,H) at 100% epiboly, collected at 1-2 s and subjected to *in situ* hybridization for *krox20/pax2.1* (A-D) or *nlz/pax2.1* (E-H). Embryos were flat-mounted with the anterior towards the top. A 5 min heat shock results in full activation of *krox20* in r2, whereas *nlz1* expression is only marginally affected. Strong activation of *nlz1* in the r2-r4 region is only observed after 20-30 min heat shock, in parallel to the repression of *krox20* in r2-r3.